OPEN ACCESS Freely available online
R. Sridhar, J. G. Tylka and E. Y. Choueiri,
"Generalized Metrics for Constant Directivity"
J. Audio Eng. Soc., vol. 67, no. 9, pp. 666–678, (2019 September.).
DOI: https://doi.org/10.17743/jaes.2019.0022

Generalized Metrics for Constant Directivity*

RAHULRAM SRIDHAR, *AES Student Member*, **JOSEPH G. TYLKA,** *AES Student Member*, **AND**
(rahulram@princeton.edu) (josephgt@alumni.princeton.edu)

EDGAR Y. CHOUEIRI, *AES Associate Member*
(choueiri@princeton.edu)

3D Audio and Applied Acoustics Laboratory, Princeton University, Princeton, NJ 08544, USA

Metrics are proposed for quantifying the extent to which a transducer's polar radiation (or sensitivity) pattern is invariant with frequency. As there is currently no established measure of this quality (often called "controlled" or "constant directivity"), five metrics, each based on commonly-used criteria for constant directivity, are proposed: (1) a Fourier analysis of sensitivity contour lines (i.e., lines of constant sensitivity over frequency and angle), (2) the average of spectral distortions within a specified angular listening window, (3) the solid angle of the frontal region with distortions below a specified threshold, (4) the standard deviation of the directivity index, and (5) cross-correlations of polar responses. These metrics are computed for 10 loudspeakers that are ranked, from most constant-directive to least, according to each metric. The resulting values and rankings are compared and the suitability of each metric for comparing transducers in different applications is assessed. For critical listening applications in reflective or dynamic listening environments, metric 1 appears most suitable, while for such applications in acoustically-treated and static environments, metrics 2 and 3 may be preferable. Furthermore, for high-amplitude applications (e.g., live sound) in reflective or noisy environments, metrics 4 and 5 appear most suitable.

0 INTRODUCTION

Many applications in audio benefit from transducers (or transducer arrays) whose directional characteristics do not vary with frequency. For example, in live sound reinforcement, it is often desirable for each loudspeaker to cover a certain region of the audience. Consequently, the loudspeaker's *coverage angle* should be constant over its usable frequency range so that no part of the audience lacks any part of the frequency spectrum [1]. Also, microphone arrays used for beamforming often attempt to isolate and capture sounds (of all frequencies) from a certain direction (or region), which requires that the spatial selectivity of the array be frequency-independent [2, 3].

Many transducer manufacturers claim to achieve "constant directivity," suggesting that the transducer's directional characteristics, or some aspect thereof, are independent of frequency (at least over some frequency range). In addition, many manufacturers also publish measured polar radiation data, generally taken in the far-field on multiple circular orbits around the transducer (cf., Toole [4, Fig. 18.6], for example), which enables the frequency dependence of that transducer's directivity to be examined and quantified. Furthermore, some research and industry groups collect similar polar radiation data, either on far-field circular orbits [5] or via extrapolation of near-field measurements [6]. However, there exists no standard measure of the degree to which a transducer exhibits constant directivity, thereby making it difficult, even when data are readily available, to evaluate manufacturers' claims and compare supposed constant-directive transducers (i.e., transducers that exhibit constant directivity).

Part of the problem is that constant directivity is often imprecisely and/or implicitly defined, whereby, for example, the polar radiation pattern of an "ideal" constant-directive loudspeaker is plotted alongside that of a real loudspeaker (cf., Geddes [7, Fig. 9], for example). The reader is then left to visually judge the degree to which the real loudspeaker's radiation pattern qualifies as constant-directive, a process that is highly subjective and prone to error. In an attempt to resolve the ambiguity surrounding this topic and facilitate the development of standardized measures of constant directivity, we seek a formal and quantifiable definition of the term.

* This article contains a generalized formulation of the metrics originally presented at the 140th Convention of the Audio Engineering Society in Paris, France (2016 May), convention paper 9501. The first and second authors contributed equally to this work.

0.1 Background and Previous Work

We refer to the *directivity* of a transducer as, generally, the extent to which its sensitivity (radiated acoustic power for loudspeakers) is biased toward a given direction. Several metrics exist to quantify directivity, the most well-known of which are the *beamwidth* (also called the coverage angle for loudspeakers) and the *directivity factor* (alternatively called the *directivity index* when expressed in dB) [8]. The coverage angle is typically defined as the angle between the −6 dB points of the main lobe [8]. As the name implies, this metric quantifies the region of space in which the radiation is largely uniform. The directivity factor, also known as the directional gain, is given by the ratio between the power radiated on-axis (or along any given reference axis) and the radiated power averaged over all directions [9]. Methods to calculate the directivity factor from a finite set of measured data have been developed [10–12, and references therein]. Another directivity metric, called the "directivity figure of merit," was proposed by Davis [13] and combines the directivity factor and the coverage angle to quantify the efficiency with which the radiated power is concentrated within the coverage angle.

Unlike for directivity, well-defined metrics do not exist for constant directivity, likely due to the lack of a standardized, quantifiable definition of the term. For example, White [1] defines constant directivity as having a constant coverage angle over a wide frequency range. Geddes [14], on the other hand, defines constant directivity as having identical (up to a scaling factor) polar response curves (presumably over a wide frequency range). However, in a later publication, Geddes [7] states that no universal definition for constant directivity exists, and so to illustrate constant directivity, one should simply publish polar response data, implying that a purely visual assessment of the data is sufficient to determine the extent to which a transducer is constant-directive. In the spirit of the work done to develop directivity metrics, we previously proposed precise definitions of, and quantitative metrics for, constant directivity [15]. However, several of these proposed metrics were only defined for polar radiation data measured on a single (horizontal or vertical) circular orbit around the transducer, and they were only evaluated using the frontal radiation data for four loudspeakers.

0.2 Objectives and Approach

The objectives of this work are: (1) to develop and characterize a suite of metrics for constant directivity that can be used to objectively evaluate and compare transducers given radiation (or sensitivity) data uniformly sampled on a sphere and (2) to establish a precise definition for constant directivity.

To these ends, we first identify, in Sec. 1, various criteria for constant directivity, which are then used to propose two definitions of the term. In Sec. 2 we present the coordinate system used in this work. We then derive, in Sec. 3, five metrics designed to quantify each previously identified criterion. In Sec. 4 we describe the application of these metrics to 10 loudspeakers, which were selected from a larger database[1] of polar radiation measurements [5]. In Sec. 5 the loudspeakers are then ranked according to each metric, and the resulting rankings are qualitatively compared with each other. We then analyze the discrepancies in the resulting rankings in order to draw insights about each metric and determine its potential advantages (or disadvantages). Finally, in Sec. 6 we summarize this work and conclude.

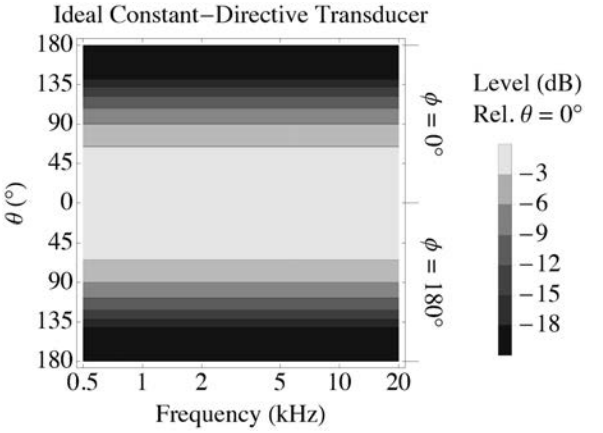

Fig. 1. Contour plot of the horizontal sensitivity pattern of an ideal constant-directive transducer according to criterion I. The angles θ and ϕ are defined in Sec. 2. Note that this plot corresponds to a full horizontal orbit around the transducer, as illustrated in Fig. 2.

1 DEFINING "CONSTANT DIRECTIVITY"

In this section we identify three criteria for constant directivity from which we propose two definitions of the term. Note that, at this point, "constant directivity" should not be considered synonymous with "directivity which is constant," as "directivity" is already defined, while "constant directivity" is not.

I. Uniformly horizontal contour lines
For a loudspeaker, a contour plot shows the loudspeaker's output level in dB, normalized by the on-axis output, as a function of both frequency and angle, with contours drawn at specific levels (e.g., −18 to 0 dB in increments of 3 dB). Based on such a plot, our first criterion for constant directivity (hereafter, simply "CD criterion") is: a transducer that exhibits constant directivity must have a contour plot in which all contour lines are perfectly horizontal [7], as shown, for example, in Fig. 1.

II. Direction-independent frequency response
In studio or live sound settings, it is often desirable for a listener at an off-axis position to receive the same spectral content as one on-axis [1], even if at a lower overall level. From this motivation, our second CD criterion is: a transducer that exhibits constant directivity must have a frequency response at any

[1] This database is available online from the 3D Audio and Applied Acoustics Laboratory at Princeton University [16].

off-axis position that is identical to its on-axis frequency response, ignoring any difference in overall level.

III. Frequency-invariant "directivity"
Finally, from the term "constant directivity," we infer that some aspect of the transducer's directional characteristics should be invariant with frequency. As defined in Sec. 0.1, "directivity" describes the directional bias in a transducer's sensitivity, a quality that is quantified by metrics such as the directivity factor and the coverage angle. By this definition and a literal interpretation of the term "constant directivity," our third CD criterion is: a transducer that exhibits constant directivity must have a directivity (or some metric thereof) which is invariant with frequency [1]. However, fulfillment of this criterion is insufficient to guarantee fulfillment of the two previous criteria, as the directivity metrics reduce the full specification of the polar radiation pattern(s) to a single spectrum. Consequently, to guarantee fulfillment of all three criteria, we turn to an alternative, and more strict, third CD criterion: a transducer that exhibits constant directivity must have polar radiation patterns that are unchanged (ignoring any differences in overall level) with frequency [14].

In view of these three criteria, we propose the following definition for constant directivity: *A transducer is said to exhibit constant directivity, over a specified frequency range, if and only if its polar radiation patterns are invariant in that range.* Furthermore, a transducer is said to be more (or less) constant-directive than another transducer, if the variations in the first transducer's polar radiation patterns are less (or more) extreme than those of the second transducer.

For some applications, the more lenient version of the third criterion may be appropriate. For example, in some beamforming applications, variations in polar radiation patterns may be tolerable provided that the directional gain (directivity factor) is constant over a specified range of frequencies. Consequently, we propose a second, more lenient definition for constant directivity: *A transducer is said to exhibit constant directivity, over a specified frequency range, if and only if its directivity factor (index) is invariant in that range.*[2,3]

2 COORDINATE SYSTEM

We adopt the spherical coordinate system given in AES56-2008 [17]. Angular coordinates $\theta \in [0, \pi]$ and $\phi \in [0, 2\pi)$ are measured such that θ indicates the angle away from on-axis (referred to as the "reference axis" in AES56-2008 [17]) along a given measurement half-plane and ϕ indicates the rotation of that half-plane around on-axis, as shown in Fig. 2.

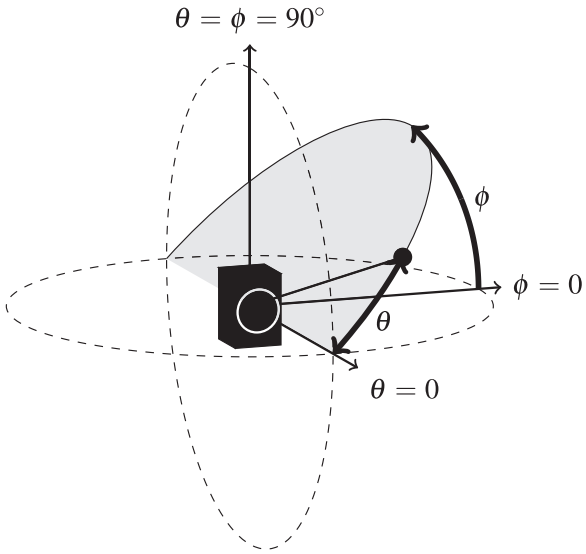

Fig. 2. Diagram of the coordinate system. The arrow perpendicular to the front face of the loudspeaker is the reference axis [17] and indicates the "on-axis" direction ($\theta = 0$). The gray semicircular disc represents a measurement half-plane and the filled black circle indicates a measurement point. The dashed circles indicate horizontal and vertical orbits.

Generally, polar radiation measurements are taken for a set of $M \times (N + 1)$ directions (θ_n, ϕ_m), for integer values of $m \in [0, M - 1]$ and of $n \in [0, N]$, where M is the number of measurement half-planes and $N + 1$ is the number of measurements taken on each half-plane. Let $\Delta\theta = \pi/N$ denote the angular spacing between neighboring measurement points on a given half-plane and $\Delta\phi = 2\pi/M$ denote the angular spacing between neighboring half-planes. The full set of measurement directions are then given by

$$(\theta_n, \phi_m) = (n\Delta\theta, m\Delta\phi). \quad (1)$$

For example, with $M = 4$ measurement half-planes, all measurement points lie along horizontal and vertical orbits (depicted by dashed circles in Fig. 2), with the half-planes corresponding to $m = 0, 2$ containing the horizontal orbit and those corresponding to $m = 1, 3$ containing the vertical orbit.

3 PROPOSED CONSTANT DIRECTIVITY METRICS

We now derive five metrics for constant directivity, each of which is based on one of the criteria identified in Sec. 1. The first metric is based on criterion I and quantifies the extent to which the contour lines are uniformly horizontal. The second and third metrics are both based on criterion II and quantify distortions in the shapes of a

[2] Alternate versions of this definition can be generated by replacing the directivity factor with another directivity metric, such as the coverage angle.

[3] Note that the proposed definitions are not mutually exclusive. In fact, satisfaction of the second definition is necessary but insufficient for satisfaction of the first, i.e., a transducer that satisfies the stricter version is also guaranteed to satisfy the lenient one, while the converse is not true.

transducer's frequency responses at off-axis positions compared to its on-axis frequency response. The last two metrics are based on the two versions of criterion III; the fourth metric quantifies the extent to which a transducer's directivity is constant with frequency, while the fifth metric quantifies the similarity (across frequency) of the transducer's polar responses.

3.1 Metric 1: Fourier Analysis of Sensitivity Contour Lines

For this metric, we first compute the frequency-dependent ratio between the sound pressure level (SPL) for each measurement direction and that for the on-axis direction. This is given in dB by

$$20\log_{10}\frac{|H_{m,n}[k]|}{|H_{0,0}[k]|},$$

where $H_{m,n}$ is the frequency response of the transducer in the direction (θ_n, ϕ_m).

For a given measurement half-plane, we generate a contour plot of these normalized magnitude responses (computed using the above expression), as is typically done in the literature (e.g., Tylka et al. [5, Fig. 1]). Here, however, we use black contour lines and color all spaces between contour lines white. The contours are drawn on a logarithmic frequency scale, over all angles in the half-plane (i.e., $n \in [0, N]$), and with a specified set of contour levels. The plot is then rasterized to a grayscale image of width V and height U (in pixels). These data are stored in a U-by-V real-valued matrix, $\mathbf{X}_m$, with elements $x_{u,v} \in [0, 1]$, where contour lines are represented by non-zero values of x and the spaces between contours are represented by zeros.

We then compute the discrete Fourier transform (DFT) along each row of the matrix to yield a complex-valued U-by-V matrix, $\mathbf{Y}_m$, with elements $y_{u,v}$. In the ideal case, where all contours are perfectly horizontal, the only non-zero values of $\mathbf{Y}_m$ will exist in the first column (i.e., all $y_{u,v\neq 0} = 0$). In less ideal cases, where the contours are not perfectly horizontal, non-zero values will exist in more than just the first column of $\mathbf{Y}_m$. Consequently, we define our metric as the percentage of the total "energy" of $\mathbf{Y}_m$ that is concentrated in the first column, given by

$$\epsilon_m = 100 \times \frac{\sum_{u=0}^{U-1} \left|y_{u,0}\right|^2}{\sum_{u=0}^{U-1}\sum_{v=0}^{V-1} \left|y_{u,v}\right|^2}. \tag{2}$$

The result is a strictly positive number $\epsilon_m \in (0, 100]$, where a value of $\epsilon_m = 100\%$ indicates that each row of $\mathbf{X}_m$ is a constant value (i.e., either it contains a complete contour or it does not) and represents a perfectly constant-directive transducer. A value of $\epsilon_m = 0$ is not possible because that would indicate that no row of $\mathbf{X}_m$ has any non-zero values (i.e., no contours exist). We then average over all M measurement half-planes, yielding

$$\epsilon = \frac{1}{M}\sum_{m=0}^{M-1}\epsilon_m. \tag{3}$$

3.2 Metric 2: Directional Average of Frequency Response Distortions

We first define the *distortion spectrum* for each measurement direction as

$$D_{m,n}[k] = \sqrt{\frac{P_{m,n}[k]}{\overline{P_{m,n}}} \Big/ \frac{P_{0,0}[k]}{\overline{P_{0,0}}}}, \tag{4}$$

where $P_{m,n}[k] = |H_{m,n}[k]|^2$ is the power spectrum in the direction (θ_n, ϕ_m) and $\overline{P_{m,n}}$ is its logarithmically-weighted average (computed using Eq. (A.14), given in Appendix A) over a given frequency range.

When the logarithm of $D_{m,n}[k]$ is taken, the distortion spectrum becomes the difference between the magnitude response in the direction (θ_n, ϕ_m) and the on-axis response, minus the change in overall (average) level. Therefore, this spectrum shows the change in the *shape* of the magnitude response, rather than the total change, thereby approximately isolating any change in perceived tonality from any change in perceived level that may occur at off-axis positions.

We then compute the *absolute* distortion spectrum, given by

$$E_{m,n}[k] = 10^{\left|\log_{10} D_{m,n}[k]\right|}, \tag{5}$$

so that relative peaks and notches contribute equally to the result. These spectra are then averaged over all directions within a given region of space (e.g., $\pm 30^\circ$ in the horizontal plane and $\pm 10^\circ$ in the vertical plane),[4] hereafter referred to as the "listening window" (cf., Toole [4, Fig. 18.6]), to yield the *listening window distortion spectrum*, given by

$$C_{\mathrm{LW}}[k] = \sqrt{\frac{\sum_{m,n} w_{m,n}\left|E_{m,n}[k]\right|^2}{\sum_{m,n} w_{m,n}}}, \tag{6}$$

where the summations are taken only over the measurement directions within the specified listening window and the weights $w_{m,n}$ (given by Eq. (B.17) in Appendix B) correspond to the surface area of the unit sphere represented by each measurement. Generally, the listening window is typically defined such that $\theta \leqslant \theta_{\mathrm{LW}}(\phi)$, where we take

$$\theta_{\mathrm{LW}}(\phi) = \sqrt{\left(\frac{\pi}{6}\right)^2\cos^2\phi + \left(\frac{\pi}{18}\right)^2\sin^2\phi}. \tag{7}$$

Hence, in the case of $M = 4$ measurement half-planes, we have $\theta_{\mathrm{LW}} = 30^\circ$ for $m = 0, 2$ (i.e., in the horizontal plane), and $\theta_{\mathrm{LW}} = 10^\circ$ for $m = 1, 3$ (vertical plane), as suggested by Toole [4].

[4] This is similar to the "direct sound," as defined by Devantier [18] as the average response over this region.

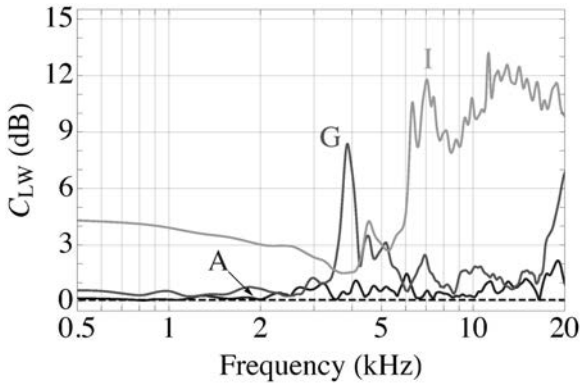

Fig. 3. Plot of C_{LW} in dB for three loudspeakers: A (black), G (dark gray), and I (light gray).

Table 1. Descriptions of the 10 loudspeakers considered in this work.

Label	Description
A	Three-way concentric studio monitor
B	Two-way concentric studio monitor
C	Three-way "controlled directivity" loudspeaker
D	Two-way studio monitor
E	Two-way studio monitor
F	Two-way bookshelf loudspeaker
G	Two-way bookshelf loudspeaker
H	Three-way bookshelf loudspeaker
I	Desktop electrostatic loudspeaker
J	Enclosed electrostatic hybrid loudspeaker with woofer

The listening window distortion spectrum may be further averaged logarithmically over frequency to yield a single number, the *average listening window distortion*, given in dB by

$$\langle C_{LW} \rangle = 10 \log_{10} \left(\overline{|C_{LW}[k]|^2} \right). \tag{8}$$

To visualize this metric, we plot C_{LW}, as computed in Eq. (6) using the listening window given in Eq. (7). One such plot is shown in Fig. 3 for three loudspeakers: A, G, and I (described in Table 1). From this plot, we see that loudspeaker A is more constant-directive in this listening window than loudspeaker G, since the listening window distortion spectrum of loudspeaker A is, in several frequency ranges, significantly smaller than that of loudspeaker G. Additionally, loudspeaker I is significantly less constant-directive than both loudspeakers A and G, since the listening window distortion spectrum of loudspeaker I is larger than the others across almost the entire frequency range.

3.3 Metric 3: Distortion Thresholding of Polar Responses

For this metric, we use the same absolute distortion spectra, $E_{m,n}[k]$, defined in Eq. (5), to determine a frequency-dependent region of the forward half of each measurement half-plane within which the distortion is below a specified threshold, E^* (e.g., $\sqrt{2}$, or 3 dB). Specifically, for a given m and for each frequency index k, we search the range $n \in [0, N/2]$ for the first (increasing from 0) threshold crossing, denoted n_m^*, such that

$$\begin{aligned} &E_{m,n}[k] \leq E^*, \text{ for all } n \leq n_m^*, \text{ and} \\ &E_{m,n}[k] > E^*, \text{ for } n = n_m^* + 1. \end{aligned} \tag{9}$$

If no such n_m^* exists because $E_{m,n}[k] \leqslant E^*$ for all $n \in [0, N/2]$, then we choose $n_m^* = N/2$. Using these threshold crossings, we then compute a frequency-dependent *constant-directive (CD) coverage solid angle*, $\Omega_{CD}[k]$, given (in sr) by

$$\Omega_{CD}[k] = 4\pi \sum_{m=0}^{M-1} \sum_{n=0}^{n_m^*} w_{m,n} \tag{10}$$

which is then logarithmically averaged over a specified frequency range to yield an average CD coverage solid angle, $\overline{\Omega_{CD}}$. Note that, since we restrict the original angle calculations to the region of space in front of the transducer (i.e., $\theta \leqslant \pi/2$), we use the forward-only corrected weights $w_{m,N/2}$, as described in Appendix B. Consequently, values for Ω_{CD} will range from 0 to 2π sr.

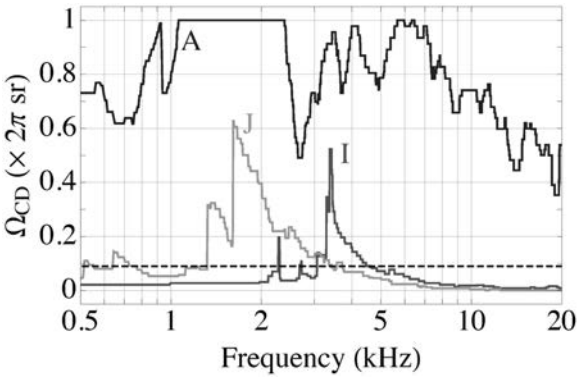

Fig. 4. Plot of Ω_{CD} for three loudspeakers: A (black), I (dark gray), and J (light gray). Note the scale on the left axis shows $\Omega_{CD}/(2\pi)$. The dashed line indicates the solid angle of the "reference" listening window defined in Eq. (7), approximately $0.9 \times 2\pi$ sr.

To visualize this metric, we plot Ω_{CD}, as shown in Fig. 4, for loudspeakers A, I, and J. We also indicate a reference value of $\Omega_{CD} \approx 0.9 \times 2\pi$ sr by the dashed line, which corresponds to the solid angle of the listening window defined in Eq. (7), as calculated using Eq. (10) for $M = 4$. The larger values of Ω_{CD} for loudspeaker A compared to loudspeakers J and I indicates that loudspeaker A exhibits a wider region within which the distortion is at most 3 dB and is therefore more constant-directive than the others.

3.4 Metric 4: Standard Deviation of Directivity Index

For this metric, we compute the logarithmically-weighted standard deviation (computed using Eq. (A.15), given in Appendix A) of the directivity index (DI) spectrum of a transducer, which is defined as the ratio of the on-axis

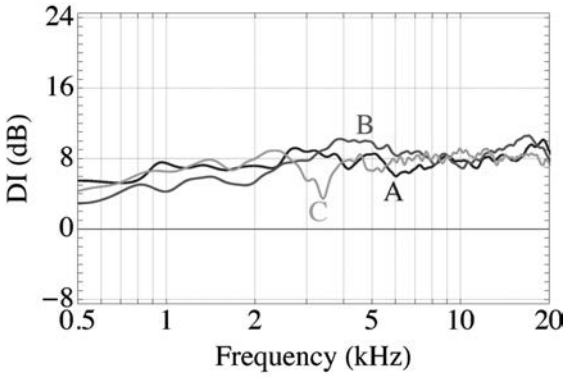

(a) Loudspeakers A (black), B (dark gray), and C (light gray)

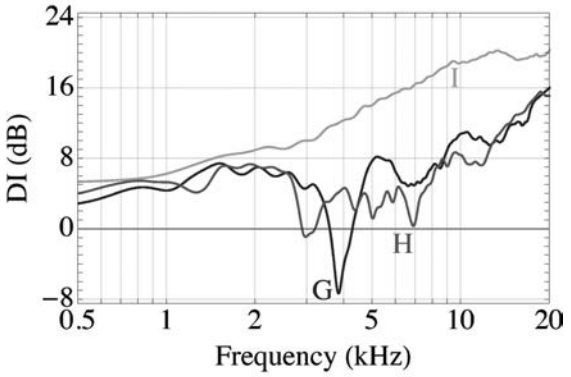

(b) Loudspeakers G (black), H (dark gray), and I (light gray)

Fig. 5. Plots of the DI spectra in dB for six loudspeakers: A–C (top panel) and G–I (bottom).

power spectrum to the average power spectrum over all directions, and is given in dB by

$$\mathrm{DI}[k] = 10\log_{10}\frac{P_{0,0}[k]}{\sum_{m,n} w_{m,n} P_{n,m}[k] / \sum_{m,n} w_{m,n}}, \tag{11}$$

where the summations are taken over all measurement directions. Note that the calculation in Eq. (11) is equivalent to that proposed by Wilson [19, 20], which is itself equivalent to the graphical method proposed by Kendig and Mueser [10].

The standard deviation, σ_{DI}, quantifies the extent to which the transducer's directivity is constant with frequency, with $\sigma_{\mathrm{DI}} = 0$ indicating that the DI is invariant with frequency. However, as discussed in Sec. 1, this does not adhere to the strictest definition of constant directivity, as a small σ_{DI} means only that the ratio between the on-axis and the average power spectra remains nearly constant with frequency, yet, in principle, the polar radiation pattern may still vary with frequency.

Fig. 5a shows the DI spectra for three loudspeakers: A, B, and C. From this plot, we see that the DI spectrum of loudspeaker C features a notch around 3.5 kHz, which should yield a larger σ_{DI} value compared to that of loudspeaker A, indicating that loudspeaker C is less constant-directive than loudspeaker A. Additionally, the range of values of the DI spectrum for loudspeaker B is approximately 2 dB greater than that of loudspeaker A, which indicates that loudspeaker B is also less constant-directive than loudspeaker A. Fig. 5b will be discussed in Sec. 5.

3.5 Metric 5: Cross-Correlation of Polar Responses

For a given measurement half-plane, we define the normalized and aligned cross-correlation (NACC), $\Phi_m[k, k']$, between two polar responses at frequency indices k and k' as

$$\Phi_m[k, k'] = \frac{\sum_{n=0}^{N} P_{m,n}[k] P_{m,n}[k']}{\left(\sum_{n=0}^{N} P_{m,n}^2[k] \sum_{n'=0}^{N} P_{m,n'}^2[k']\right)^{0.5}}, \tag{12}$$

for $k, k' \in [0, K/2]$, where K is the number of points in each power spectrum (and so $K/2$ corresponds to the Nyquist frequency). Using the above definition for Φ_m, we compute the NACC between pairs of polar responses for every combination of frequencies. We then average over all M measurement half-planes, yielding

$$\Phi[k, k'] = \frac{1}{M} \sum_{m=0}^{M-1} \Phi_m[k, k']. \tag{13}$$

For each frequency pair (k, k'), we then have one NACC value.[5] We then write $\Phi[k, k']$ as a square matrix with $K/2 + 1$ rows and columns, where all elements along the main diagonal are always equal to unity and the matrix is necessarily symmetric. This matrix is visualized as shown in Fig. 6 for three loudspeakers: A, G, and J. We see, for each plot, that the NACC values along the diagonal from the bottom left to the top right corners of each plot are identically 1 (indicated by the white color). Furthermore, since the plot for loudspeaker A is largely white, whereas that for loudspeaker J has significant regions of low NACC values (indicated by the black color), we conclude that loudspeaker A is more constant-directive than G. For loudspeaker G, we see a narrowband region of low NACC values around 4 kHz, corresponding to a polar radiation pattern that is particular to that frequency range (i.e., one that is not similar to the radiation pattern for that loudspeaker at any other frequency).

We also compute an average NACC value by computing a logarithmically-weighted mean over a specified frequency range, first across columns and then across rows. This average value, $\overline{\overline{\Phi}}$, can range from 0 to 1, with a value of

[5] An alternative but similar calculation is to compute a two-dimensional NACC, in which a three-dimensional polar radiation pattern at a given frequency (represented mathematically by a matrix of polar responses) is cross-correlated with another such radiation pattern at a different frequency.

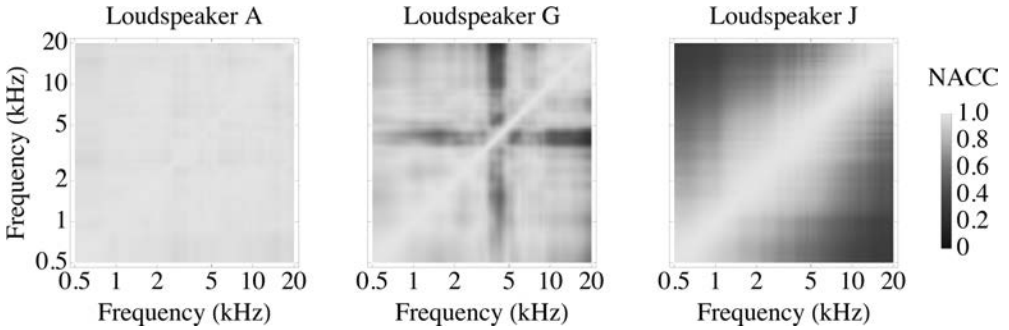

Fig. 6. Normalized and aligned cross-correlation (NACC) matrices for the forward horizontal radiation of three loudspeakers: A (left panel), G (center), and J (right).

1 indicating that the transducer's polar responses in that frequency range are all identical.

4 EXPERIMENTAL EVALUATION OF METRICS

To evaluate the metrics proposed in the previous section, we compute each of them using the polar radiation data for 10 loudspeakers, which were selected from a database of loudspeaker polar radiation measurements [5]. The data are available as impulse responses, measured in an anechoic chamber, for the horizontal and vertical measurement half-planes only ($M = 4$), with an angular resolution of $\Delta\theta = 5^\circ$ ($N = 37$). Descriptions of the selected loudspeakers are provided, in brief, in Table 1. The metrics proposed here have also been computed and published online for the entire database [16].

For metric 1, we generate contour plots over the frequency range from 500 Hz to 20 kHz, with contour lines drawn from −18 dB to −3 dB in increments of 3 dB, and convert the plot to an image with a width of $V = 64$ pixels and a height of $U = 32$ pixels.[6] For metric 2 we define the listening window given in Eq. (7). For metric 3 we use a distortion threshold of 3 dB. All frequency-domain averages are performed over the range 500 Hz to 20 kHz.[7]

5 RESULTS AND DISCUSSION

The calculated values for each metric and for each loudspeaker are shown in Table 2, and the rankings, from most constant-directive to least, according to each metric, are shown in Table 3. To give the values for each metric a sense of scale, we also compute the value corresponding to 10% of the total range (i.e., max −min) of the values in each column of Table 2, which we list in the bottom row of that table. Below, we compare these values and discuss the apparent behavior and potential advantages (or disadvantages) of each metric.

Table 2. Calculated values of the five constant directivity metrics for each of the 10 loudspeakers (labeled A–J) used in this analysis. The bottom row shows the value corresponding to 10% of the total range (i.e., max −min) of the values in each column.

Label	ϵ (%)	$\langle C_{\mathrm{LW}} \rangle$ (dB)	$\overline{\Omega_{\mathrm{CD}}}$ ($\times 2\pi$ sr)	σ_{DI} (dB)	$\overline{\overline{\Phi}}$
A	48.39	0.48	0.80	1.12	0.98
B	45.74	0.51	0.62	2.18	0.96
C	49.31	0.83	0.61	1.28	0.95
D	47.34	0.95	0.60	2.28	0.92
E	45.63	0.97	0.60	2.61	0.92
F	44.18	1.10	0.60	2.64	0.92
G	45.44	1.67	0.52	3.74	0.87
H	43.28	4.04	0.47	3.36	0.86
I	42.98	7.18	0.05	5.24	0.85
J	33.70	15.18	0.10	6.97	0.75
10%	1.56	1.47	0.08	0.59	0.02

Table 3. The 10 loudspeakers (labeled A–J) used in this analysis ranked, from most constant-directive (rank 1) to least (rank 10), according to each of the five metrics.

Rank	ϵ	$\langle C_{\mathrm{LW}} \rangle$	$\overline{\Omega_{\mathrm{CD}}}$	σ_{DI}	$\overline{\overline{\Phi}}$
1	C	A	A	A	A
2	A	B	B	C	B
3	D	C	C	B	C
4	B	D	D	D	D
5	E	E	E	E	E
6	G	F	F	F	F
7	F	G	G	H	G
8	H	H	H	G	H
9	I	I	J	I	I
10	J	J	I	J	J

5.1 Metric 1

We first observe that the ranking generated by metric 1 (ϵ) is noticeably different from those generated by the other four metrics. To explain this discrepancy, we make two observations by comparing the contour plots of loudspeakers B and C, which are shown in Fig. 7. First, we note that

[6] We intentionally choose such a low-resolution image so as to "blur" the contour lines, thereby reducing the sensitivity of the computed metric to minor fluctuations in the contour lines. We expect this to correspond better with evaluations of constant directivity based on a purely visual analysis of the contour plot, because such an analysis is likely to involve some visual averaging.

[7] A lower frequency limit of 500 Hz is used because the anechoic chamber in which the directivity measurements are made is anechoic only down to approximately 425 Hz [5].

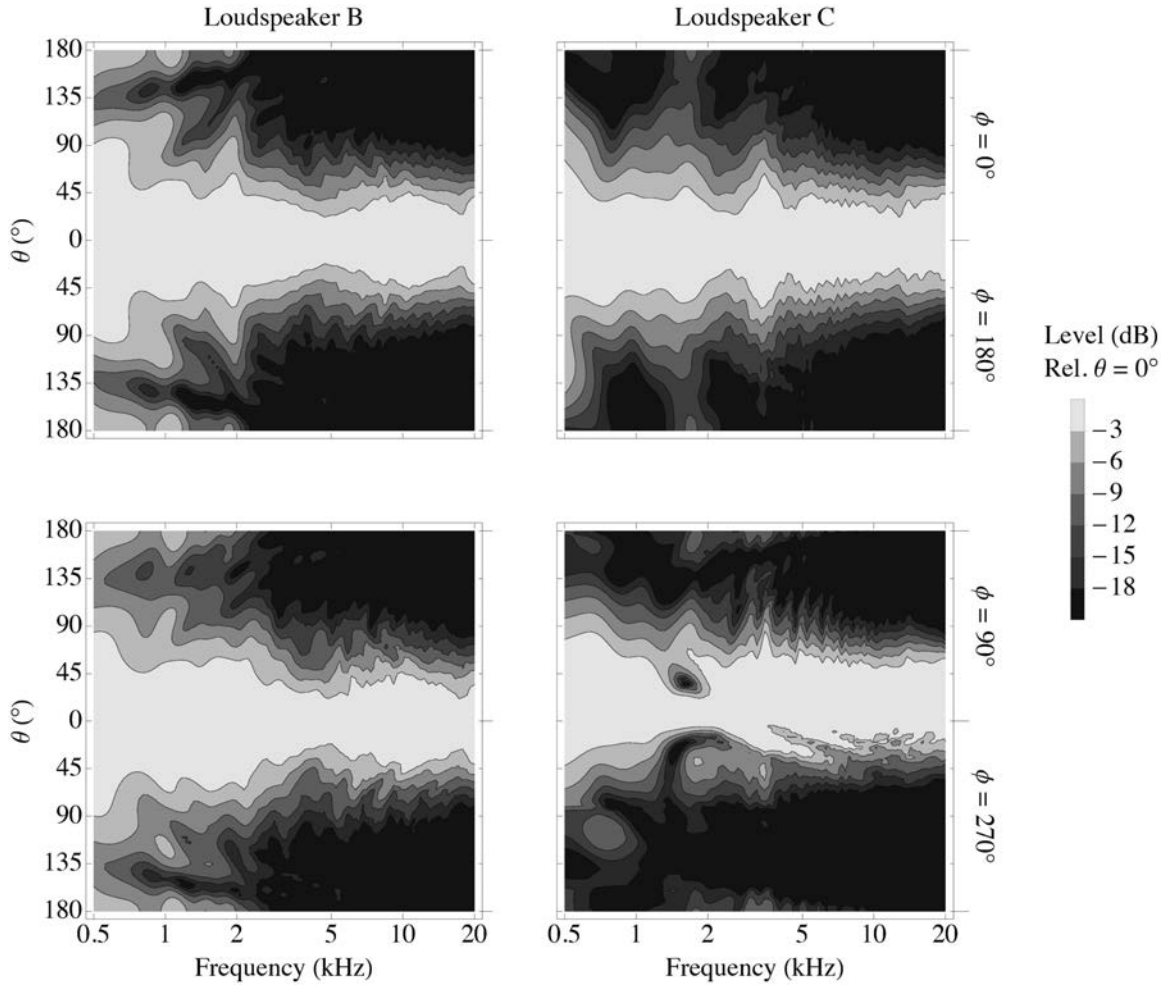

Fig. 7. Contour plots of horizontal (top row) and vertical (bottom) radiation for loudspeakers B (left column) and C (right). Each plot shows level normalized by the respective loudspeaker's on-axis response.

loudspeaker B radiates more energy backwards (i.e., $\theta \geqslant 90^\circ$) for frequencies below ∼2 kHz than does loudspeaker C. The directivity of this backwards radiation is not very constant, as evidenced, for example, by the looping contour lines. Second, we note the presence of deep notches between 1 and 2 kHz in the forward radiation section ($\theta \leqslant 90^\circ$) of the vertical contour plot for loudspeaker C. These two observations suggest that metric 1 penalizes the larger backwards radiation by loudspeaker B more so than it does the deep notches exhibited by loudspeaker C. We expect this to be true even if the backwards radiation is low-amplitude (as is the case here), since, by construction, metric 1 does not differentiate between contour lines based on level.

In contrast, the values of $\overline{\overline{\Phi}}$ (metric 5) for loudspeakers B and C are quite similar (see Table 2). This suggests that metric 5 does not penalize low-amplitude deviations, whereas metric 1 appears to treat all regions of the contour plot and all contour levels equally. Due to this sensitivity to changes in low-amplitude and backwards radiation, we may use metric 1 to better distinguish between loudspeakers D, E, and F, whereas the other four metrics produce very similar values (relative to the 10% values listed in the bottom row of Table 2). Thus, for applications in which low-amplitude deviations in directivity, even in the backwards radiation region, is undesirable, metric 1 might be the best option for comparing the extent to which different loudspeakers exhibit constant directivity. However, for applications in which such deviations are irrelevant, metric 1 may produce biased results unless steps are taken to modify it (e.g., by excluding backwards radiation or by weighting differently the contour lines for different levels).

5.2 Metric 2

Recall that, by construction, $\langle C_{\mathrm{LW}} \rangle$ (metric 2) only takes into account spectral distortions within a predefined listening window, the solid angle of which, in our case, is approximately $0.09 \times 2\pi$ sr. As all of the Ω_{CD} (metric 3) values for loudspeakers A–H are well over $0.1 \times 2\pi$ sr, the consistently low values (<3 dB, approximately) of $\langle C_{\mathrm{LW}} \rangle$ are to be expected. We also see that, while the change in metric 3 between loudspeakers A and B appears significant, the corresponding change in metric 2 is not. This may be explained by the low-distortion region for each loudspeaker being larger than the reference listening window, such that neither loudspeaker produces much distortion within that

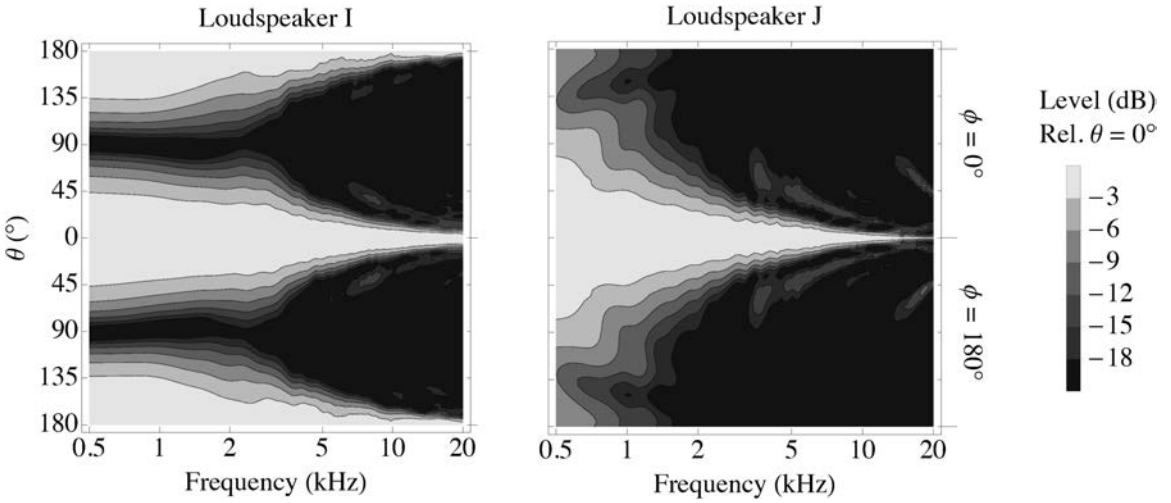

Fig. 8. Contour plots of horizontal radiation for loudspeakers I (left panel) and J (right).

window. Consequently, one apparent limitation of metric 2 is that it cannot measure improvements in constant directivity if they occur outside of the predefined listening window. However, if the listening window is chosen appropriately for a given application, this may be an ideal metric.

5.3 Metric 3

In Table 3 we see that metric 3 is the only metric to rank loudspeaker J above loudspeaker I. As shown in Fig. 4, it is clear that indeed loudspeaker J has a slightly larger region of low distortion. However, all of the other metrics produce significantly different values for loudspeaker I than for J (see Table 2). For example, we see that the value of metric 2 for loudspeaker J is 8 dB larger than that for loudspeaker I, which suggests that loudspeaker I is significantly more constant-directive than J. By construction, however, metric 3 relies on a 3 dB distortion threshold, such that it cannot take into account any variations in distortion beyond that threshold.

It is also worth noting that metric 3 is the only metric to produce comparable values for both electrostatic loudspeakers (I and J). This suggests that metric 3 is less sensitive to changes in the directivity of highly directive loudspeakers than of less directive ones. Furthermore, we expect that the directivity of the loudspeaker will tend to put a lower bound on the value of metric 3. For example, a loudspeaker whose −3 dB coverage pattern (i.e., the horizontal coverage angle × the vertical coverage angle) is at least 60° × 60° at all frequencies will necessarily have a CD coverage solid angle that includes at least that entire region.

Given this consideration, a useful extension to this metric might be to normalize a loudspeaker's Ω_{CD} by the solid angle of its coverage pattern. This may be a more useful metric for comparing two loudspeakers when one of them has a coverage pattern that is, for example, twice the size of the other's and also twice the CD coverage solid angle. As originally defined, metric 3 would suggest that one loudspeaker is twice as constant-directive as the other. However, as most listening would typically take place within their respective coverage areas, these two loudspeakers may actually be comparably constant-directive for their intended uses. We do not consider such a metric in this work as, strictly speaking, it would no longer be a measure of constant directivity, but instead a combined measure of constant directivity and directivity.

5.4 Metric 4

In addition to metric 1, metric 4 (σ_{DI}) is the only other metric that ranks loudspeaker C above B. We see in Fig. 7, that for frequencies below ∼3 kHz, the directivity of loudspeaker B is comparatively smaller, especially in the vertical plane, while above this frequency the radiation patterns of these loudspeakers are similar (see also plots of the DI spectra in Fig. 5a). This yields a larger standard deviation of the directivity index for loudspeaker B than for C, resulting in B being ranked below C, despite the notches in the vertical contour plot and in the DI spectrum of loudspeaker C. A similar effect is shown even more dramatically in Fig. 5b. From this figure, it is clear that loudspeaker G is less constant-directive than H, but loudspeaker I compared to G is less obvious, as G features a deep narrowband notch in its DI spectrum, while loudspeaker I exhibits a broadband trend in which its DI increases by 15 dB. As shown in Table 2, the value of σ_{DI} for loudspeaker G is only slightly larger than that for H, whereas for loudspeaker I, the value is significantly larger (compared to H), suggesting that metric 4 penalizes broadband spectral trends in directivity more severely than narrowband deviations.

Despite similarities in their rankings of certain loudspeakers, metrics 1 and 4 disagree in terms of the relative magnitudes of their changes between those loudspeakers. As shown in Table 2, from loudspeaker I to J there is a more significant decrease in the value of metric 1 compared to the increase in the value of metric 4. Additionally, the change in the values of each of these two metrics from loudspeakers G to I is comparable (to that from I to J) for metric 4, but significantly smaller for metric 1. To explain this discrepancy, we examine the horizontal contour plots for loudspeakers I and J, which are shown in Fig. 8. It is apparent from these plots that, up to ∼4 kHz, the directivity

of loudspeaker I is more constant than that of J because the contour lines for the former are generally more horizontal compared to those of the latter.

From this, we infer that metric 1 tends to quantify the fraction of the contour lines that are horizontal, even if they are only horizontal over a specific frequency band, rather than the extent to which the contour lines are horizontal overall. Therefore, metric 1 may be biased in favor of loudspeakers that are not constant-directive over the entire frequency range (such as loudspeaker I), provided that they have some wide sections of largely horizontal contour lines. Metric 4, on the other hand, appears to quantify the overall variation in directivity, allowing it to more comprehensively assess the extent to which a loudspeaker is constant-directive over the *entire* frequency range (500 Hz to 20 kHz in this case).

5.5 Metric 5

From Table 3 we notice that metric 5 obtains the same ranking (alphabetical ordering) as metric 2. This is somewhat surprising since we know that metric 2, by definition, only considers the distortion in a narrow listening window, whereas metric 5 takes into account the entire polar response. However, as seen in Eq. (12), the calculation of metric 5 effectively attributes a greater weight to larger polar response values, which typically occur within the listening window, and ignores smaller values, which tend to occur outside of the listening window. Thus, both metrics might effectively end up focusing on the listening window region. The relative magnitudes of the changes in the values of each metric between adjacent loudspeakers, however, do not always agree. For example, the changes in metric 2 from G to H, and from H to I are both rather large ($\sim$3 dB), whereas for metric 5, these changes are comparatively small ($\sim$0.01). Consequently, these metrics may only be in agreement due to the choice of these particular 10 loudspeakers.

It is worth noting that metrics 4 and 5 (both based on criterion III), not only rank the loudspeakers in very similar orders, but also have values that exhibit a similar trend (see Table 2). This finding corroborates the claim made in Sec. 1, that frequency-invariant polar radiation patterns necessarily entail a constant directivity index, since an increasing NACC value correlates with a decreasing standard deviation of the directivity index.

6 SUMMARY AND CONCLUSIONS

Motivated by the lack of a precise, standardized definition of constant directivity and of metrics that quantify the extent to which a transducer exhibits that quality, we derived a set of five metrics, each of which satisfies one or more of three criteria for constant directivity specified in Sec. 1. These criteria were also used to define the term "constant directivity" as either a characteristic of a transducer whose polar radiation patterns are invariant across a specified range of frequencies, or, more leniently, as a transducer whose directivity factor (or index) is invariant with frequency.

The first metric we proposed involves a Fourier analysis of sensitivity contour lines (i.e., lines of constant sensitivity over frequency and angle), and is based on the first criterion for constant directivity that requires that a transducer exhibiting constant directivity (i.e., a constant-directive transducer) have a contour plot with all contour lines perfectly horizontal. The second and third metrics are based on the second criterion that requires that constant-directive transducers demonstrate minimal distortion in their off-axis frequency response. Metric 2 is computed by averaging frequency response distortions over a specified range of directions, while metric 3 is computed by distortion-thresholding polar responses to determine an angular region of low-distortion. The fourth and fifth metrics are based on the third criterion, which requires that the directivity of the transducer be invariant with frequency, or more strictly, that the polar radiation pattern of the transducer remain unchanged with frequency, with satisfaction of the latter variant guaranteeing satisfaction of the former (see Sec. 1). Metric 4 is computed by taking the standard deviation of the directivity index and metric 5 is computed by averaging the normalized and aligned cross-correlation (NACC) of polar responses.

To evaluate these metrics, we computed the value of each metric using the measured polar radiation data of 10 loudspeakers, the details of which are presented in Sec. 4 (also see Table 1). We then ranked these loudspeakers, from most constant-directive to least, according to each metric, and subsequently compared the resulting values and rankings. From these comparisons (discussed in Sec. 5), we draw the following insights regarding the suitability of each metric for comparing transducers based on the extent to which each exhibits constant directivity:

1. Metric 1 may be the most suitable for critical listening applications in reflective environments or in which the listening position is not defined a priori, as it tends to treat all regions of the contour plot and all contour levels equally (see Sec. 5.1). This is desirable since, under such conditions, all aspects of a loudspeaker's radiation may affect the listener's experience.
2. Metrics 2 and 3 are likely the most suitable for critical listening applications in quiet, acoustically-treated environments with a relatively static listener, since, by construction, metric 2 is insensitive to variations in spectral distortions outside the predefined listening window (Sec. 5.2), and metric 3 is similarly insensitive to those beyond the predefined distortion threshold (Sec. 5.3).
3. For live sound or other high-amplitude applications in reflective or noisy environments, metrics 4 and 5 are likely the most suitable since metric 4 tends to ignore narrowband deviations in directivity (Sec. 5.4) and metric 5 largely ignores any changes in low-amplitude polar responses (Sec. 5.5), both of which

may not be perceptually relevant due to masking effects.

Given these insights, we conclude that all of the metrics proposed in this work may be suitable for standardization, although each may be best suited to a different application.

Note that, although not explicitly considered here, we expect all of the proposed metrics to be applicable to many types of transducers, including microphones and arrays (of loudspeakers or of microphones). Additionally, while the metrics proposed here are all defined for three-dimensional radiation data measured in multiple planes (horizontal and vertical, at least), we expect the specialization of these metrics to more restricted datasets (e.g., frontal horizontal radiation alone) to be straightforward. This type of specialization was done, for example, in our original paper [15] on this work and in an earlier work on the directivity index [21]. However, as all of the proposed metrics are defined using polar radiation data measured on equally-spaced angular grids, a useful extension of this work would be to generalize the proposed metrics for use with data measured on arbitrary grids.

7 ACKNOWLEDGMENTS

This work was sponsored by the Sony Corporation of America. The authors would like to thank L. Mosakowski, T. Matchen, T. Jin, G. Colombi, and M. Hamati for their contributions to this project, and the anonymous reviewers for their feedback on an earlier draft of this manuscript.

8 REFERENCES

[1] J. White, "The Constant Directivity White Horn White Paper," in *The PA Bible*, Addition 6, Electro-Voice, Inc. (1980). https://www.electrovoice.com/binary/EV_PABible-07-Add06-Constant_Directivity_White_Horn_Paper-1980.pdf

[2] M. Van der Wal, E. W. Start, and D. de Vries, "Design of Logarithmically Spaced Constant-Directivity Transducer Arrays," *J. Audio Eng. Soc.*, vol. 44, pp. 497–507 (1996 Jun.). http://www.aes.org/e-lib/browse.cfm?elib=7894

[3] D. B. Ward, R. A. Kennedy, and R. C. Williamson, "Constant Directivity Beamforming," in M. Brandstein and D. B. Ward (eds.) *Microphone Arrays. Digital Signal Processing* (Springer, Berlin, Heidelberg, 2001). https://doi.org/10.1007/978-3-662-04619-7_1

[4] F. E. Toole, "Chapter 18 - Loudspeakers II: Objective Evaluations," in F. E. Toole (ed.) *Sound Reproduction* (Focal Press, 2007). https://doi.org/10.1016/B978-0-240-52009-4.50023-X

[5] J. G. Tylka, R. Sridhar, and E. Choueiri, "A Database of Loudspeaker Polar Radiation Measurements," presented at the *139th Convention of the Audio Engineering Society* (2015 Oct.), e-Brief 139. http://www.aes.org/e-lib/browse.cfm?elib=17906

[6] W. Klippel and C. Bellmann, "Holographic Nearfield Measurement of Loudspeaker Directivity," presented at the *141st Convention of the Audio Engineering Society* (2016 Sep.), convention paper 9598. http://www.aes.org/e-lib/browse.cfm?elib=18402

[7] E. R. Geddes, "Directivity in Loudspeaker Systems," GedLee, LLC White Paper (2009). http://www.gedlee.com/Papers/directivity.pdf

[8] D. Davis E.Jr. Patronis, and P. Brown, "Sound System Engineering," Fourth Ed. (Focal Press, 2013).

[9] C. T. Molloy, "Calculation of the Directivity Index for Various Types of Radiators," *J. Acoust. Soc. Amer.*, vol. 20, no. 4, pp. 387–405 (1943 Jul.). https://doi.org/10.1121/1.1906390

[10] P. M. Kendig and R. E. Mueser, "A Simplified Method for Determining Transducer Directivity Index," *J. Acoust. Soc. Amer.*, vol. 19, no. 4, pp. 691–694 (1947 Jul.). https://doi.org/10.1121/1.1916539

[11] D. Davis, "A Proposed Standard Method of Measuring the Directivity Factor 'Q' of Loudspeakers Used in Commercial Sound Work," *J. Audio Eng. Soc.*, vol. 21, pp. 571–578 (1973 Sep.). http://www.aes.org/e-lib/browse.cfm?elib=1948

[12] M. A. Gerzon, "Calculating the Directivity Factor γ of Transducers from Limited Polar Diagram Information," *J. Audio Eng. Soc.*, vol. 23, pp. 369–373 (1975 Jun.). http://www.aes.org/e-lib/browse.cfm?elib=2688

[13] D. Davis, "Establishing a Loudspeaker's Directivity Figure of Merit (DFM)," presented at the *54th Convention of the Audio Engineering Society* (1976 May), convention paper 1117. http://www.aes.org/e-lib/browse.cfm?elib=2297

[14] E. R. Geddes, "Source Radiation Characteristics," *J. Audio Eng. Soc.*, vol. 34, pp. 464–478 (1986 Jun.). http://www.aes.org/e-lib/browse.cfm?elib=5263

[15] R. Sridhar, J. G. Tylka, and E. Choueiri, "Metrics for Constant Directivity," presented at the *140th Convention of the Audio Engineering Society* (2016 May), convention paper 9501. http://www.aes.org/e-lib/browse.cfm?elib=18200

[16] R. Sridhar and J. G. Tylka, "Loudspeaker Directivity: An Ongoing Experimental Survey," *3D Audio and Applied Acoustics Laboratory,* Princeton University (2015 Sep.). [Online; accessed 2-May-2019]. https://www.princeton.edu/3D3A/Directivity.html

[17] AES56-2008: AES standard on acoustics - Sound source modeling - Loudspeaker polar radiation measurements," Audio Engineering Society, Inc. (2008, reaffirmed 2014). http://www.aes.org/publications/standards/search.cfm?docID=72

[18] A. Devantier, "Characterizing the Amplitude Response of Loudspeaker Systems," presented at the *113th Convention of the Audio Engineering Society* (2002 Oct.), convention paper 5638. http://www.aes.org/e-lib/browse.cfm?elib=11234

[19] G. L. Wilson, "Directivity Factor: Q or R_θ? Standard Terminology and Measurement Methods," *J. Audio Eng. Soc.*, vol. 21, pp. 828, 830, 833, (1973 Dec.). http://www.aes.org/e-lib/browse.cfm?elib=10298

[20] G. L. Wilson, "More on the Measurement of the Directivity Factor," *J. Audio Eng. Soc.*,

vol. 22, pp. 180, 182, (1974 Apr.). http://www.aes.org/e-lib/browse.cfm?elib=2771

[21] J. G. Tylka, and E. Choueiri, "On the Calculation of Full and Partial Directivity Indices," *3D Audio and Applied Acoustics Laboratory*, Princeton University (2014 Nov.). http://www.princeton.edu/3D3A/Publications/Tylka_3D3A_DICalculation.pdf

APPENDIX A LOGARITHMICALLY-WEIGHTED MEAN AND VARIANCE

Consider a discrete spectrum $X[k]$ for $k \in [0, K-1]$, where the frequency index, k, is proportional to the frequency in Hz, given by kF_s/K, and F_s is the sampling rate. We define the logarithmically-weighted average, $\overline{X}$, over the frequency index range $[K_1, K_2]$, as a weighted average

$$\overline{X} = \frac{\sum_{k=K_1}^{K_2} \frac{1}{k} \cdot X[k]}{\sum_{k=K_1}^{K_2} \frac{1}{k}}. \tag{A.14}$$

Similarly, we define the logarithmically-weighted variance σ_X^2 by

$$\sigma_X^2 = \frac{\sum_{k=K_1}^{K_2} \frac{1}{k} \left(X[k] - \overline{X}\right)^2}{\sum_{k=K_1}^{K_2} \frac{1}{k}}. \tag{A.15}$$

APPENDIX B DIRECTION-DEPENDENT WEIGHTS

In this appendix we adopt the direction-dependent weights given by Tylka and Choueiri [21]. Consider a plane perpendicular to on-axis (see Fig. 2) at some distance $z \in [-1, 1]$ from the origin. The intersection of this plane and the unit sphere defines a circle (or a point if $|z| = 1$) consisting of all directions which satisfy $z = \cos\theta$. The surface area of the portion of the unit sphere (i.e., the solid angle) for which $z \geqslant \cos\theta$ is given by

$$\Omega_0(\theta) = \int_{\phi=0}^{2\pi} \int_{\theta'=0}^{\theta} \sin\theta' d\theta' d\phi = 2\pi(1 - \cos\theta), \tag{B.16}$$

where θ' is a variable of integration and Ω_0 is given in sr.

We use Eq. (B.16) to compute weights that correspond to the surface area of the unit sphere represented by each measurement direction, angular coordinates for which are given in Eq. (1). These weights are given by

$$w_{m,n} = \begin{cases} \dfrac{\Omega\left(\frac{\Delta\theta}{2}, 0\right)}{4\pi M} & \text{for } n = 0, \\ \dfrac{\Omega\left(\pi, \pi - \frac{\Delta\theta}{2}\right)}{4\pi M} & \text{for } n = N, \\ \dfrac{\Omega\left((n + \frac{1}{2})\Delta\theta, (n - \frac{1}{2})\Delta\theta\right)}{4\pi M} & \text{otherwise,} \end{cases} \tag{B.17}$$

where we have let

$$\Omega(\alpha, \beta) = \Omega_0(\alpha) - \Omega_0(\beta). \tag{B.18}$$

In the above equations, each weight is divided by M since the surface area must be evenly split between corresponding points from each measurement half-plane.

When restricting ourselves to forward radiation, we consider only those measurements where $n \in [0, N/2]$, and impose a correction to the direction-dependent weights by assigning $0.5\, w_{m,N/2}$ to the corresponding end-point measurements. Note that the weights derived in this appendix are proportional to those provided by Wilson [20, Table I], where the weights are normalized such that they differ from ours by a factor of $2M$ exactly.

THE AUTHORS

Rahulram Sridhar

Joseph G. Tylka

Edgar Y. Choueiri

Rahul Sridhar is a Ph.D. student in the Department of Mechanical and Aerospace Engineering and an Assistant in Research in the 3D Audio and Applied Acoustics (3D3A) Laboratory, where he is conducting research on the individualization of head-related transfer functions for 3D sound reproduction. Rahul's research interests include 3D audio, psychoacoustics, and digital signal processing.

•

Joe Tylka is a recent Ph.D. recipient from the 3D Audio and Applied Acoustics Laboratory at Princeton University, where his dissertation research explored binaural rendering and virtual navigation of recorded 3D sound fields. Joe's research interests include machine listening and acoustic signal processing.

•

Edgar Choueiri is a professor of applied physics at the Mechanical and Aerospace Engineering department of Princeton University and associated faculty at the Department of Astrophysical Sciences. He heads Princeton's Electric Propulsion and Plasma Dynamics Lab and the 3D Audio and Applied Acoustics Lab. Edgar's research interests include plasma physics, plasma propulsion, acoustics, and 3D audio.